

Notes

Effect of Architecture on the Crystal Morphology of Block Copolymers. Small-Angle X-ray Scattering and Differential Scanning Calorimetry

Chiraphon Chaibundit, Withawat Mingvanish, and Colin Booth

Department of Chemistry, University of Manchester, Manchester M13 9PL, UK

Shao-Min Mai,* Simon C. Turner, J. Patrick A. Fairclough, and Anthony J. Ryan

Department of Chemistry, University of Sheffield, Sheffield S3 7HF, UK

Polycarpos Pissis

Physics Department, National Technical University of Athens, Zografou Campus, 15780 Athens, Greece

Received February 1, 2002

Revised Manuscript Received March 22, 2002

Introduction

Recently, we have synthesized a number of block copolymers of ethylene oxide and 1,2-butylene oxide with diblock (E_mB_n) and triblock ($B_nE_mE_n$ and $E_mE_nE_m$) architectures. We use E to denote an oxyethylene unit, OCH_2CH_2 , B to denote an oxybutylene unit, $\text{OCH}_2\text{CH}(\text{C}_2\text{H}_5)$, and m and n to denote number-average block lengths in chain units. The majority of the copolymers were made primarily for study of microphase separation and structure in the melt state.¹ However, the stereoregular E-blocks of the copolymers can crystallize while the atactic B-block cannot, and we have taken the opportunity to investigate the crystal morphology of the copolymers via lamellar spacings from small-angle X-ray scattering (SAXS) and enthalpies of fusion and melting temperatures from differential scanning calorimetry (DSC).

The number-average molar masses of the samples available are in the range $M_n = 1600\text{--}16\,000\text{ g mol}^{-1}$ with compositions in the range 24–87 wt% E. Our previous work on the crystallization of these samples has been largely focused on the diblock copolymers.^{2–6} Specific effects of melt structure on crystallization have been reported, including an epitaxial relationship between domain spacings in diblock copolymers quenched from hexagonal melts,³ preferred orientation effects in crystallization of a diblock copolymer from a presheared gyroid melt,⁵ and containment of crystallization within the cylindrical and spherical E-block domains of hexagonal and cubic phases of blends of diblock copolymers with B homopolymers.⁶ An analysis of SAXS data in terms of lamellae comprising either disordered and ordered (crystal) layers (normal density model) or two ordered layers (liquid crystal/crystal model) favored the

former for the longer chains (contour length $> 500\text{ \AA}$) and the latter for shorter chains.⁴

Coming to the crystallization of the triblock copolymers, interest lies mainly in the behavior of the BEB copolymers. This is because the noncrystalline end blocks may obstruct the annealing process which is important in the crystallization of polymers and which leads to lamellar thickening. Indeed, annealing has been used to obtain equilibrium structures (for short chains) and near-equilibrium structures (for longer chains) in our work on diblock copolymers.⁴ The purpose of this note is to record our observation that the crystallization of BEB copolymers does indeed differ from that of EBE copolymers and that effects are seen clearly in results from thermal analysis as well as in the lamellar spacing itself.

Experimental Section

Samples. The diblock and triblock copolymers used (see ref 1 for listings: data for copolymers $B_4E_{37}B_4$, $B_5E_{39}B_5$, and $B_{14}E_{40}B_{14}$ are also included) were prepared by sequential oxyanionic polymerization as described previously.^{4,7} The chain length distributions of the EB and BEB copolymers (from GPC) were narrow, $M_w/M_n < 1.05$, while those of the EBE copolymers were wider, $M_w/M_n < 1.2$, this being a consequence of the slow reaction of ethylene oxide with the secondary oxyanion of their B-block precursor.^{7,8} End and chain group analysis via ^{13}C NMR spectroscopy gave the average molecular formulas and confirmed the block architecture and sample purity. After preparation the copolymers were cooled slowly from the melt to room temperature (ca. $1\text{ }^\circ\text{C min}^{-1}$) and then stored in a freezer ($-20\text{ }^\circ\text{C}$) until use in SAXS and DSC. Certain samples investigated by SAXS (but not by DSC) were recrystallized from self-seeded melts at temperatures less than $2\text{ }^\circ\text{C}$ below their melting points. This method was used for obtaining unfolded poly(ethylene glycol)s ($l \approx 250\text{--}600\text{ \AA}$) by Buckley and Kovacs.⁹

X-ray Scattering. Measurements were carried out on beamline 8.2 of the SRS at the CCLRC Daresbury Laboratory, Warrington, UK. The camera enabled simultaneous recording of wide-angle X-ray scattering (WAXS) and SAXS patterns. Samples were sealed into DSC pans and mounted on a Linkham DSC stage, which allowed adjustment of temperature. Experimental data were corrected for background scattering (subtraction of the scattering from the camera, hot stage, and an empty cell) and for any departure from positional linearity of the detectors. Details of the method, including calibration, can be found elsewhere.^{4,10}

Differential Scanning Calorimetry. A Perkin-Elmer DSC-7 instrument was used. Samples were sealed into aluminum pans and cooled to $10\text{ }^\circ\text{C}$ before heating at $2\text{ }^\circ\text{C min}^{-1}$. The temperature at the peak of the endotherm (T_{pk}) and the peak area were used to obtain the melting temperature (T_m) and the enthalpy of fusion ($\Delta_{fus}H$). The temperature and power scales of the calorimeter were calibrated by melting indium, and the temperature scale in the range of interest was checked by melting organic standards. Thermal lag was determined by melting standards at different heating rates (s) and linearly extrapolating T_{pk} against $s^{1/2}$ to zero heating rate, i.e., to the true values of T_m .

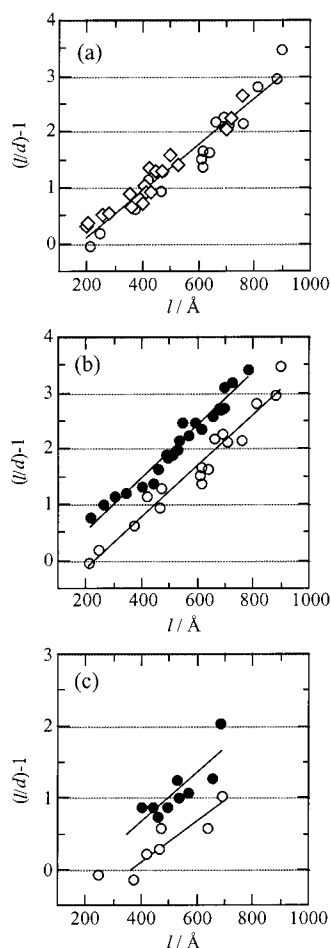


Figure 1. Ratio of molecular length (l) to lamellar spacing from SAXS (d) in the form $(l/d) - 1$ plotted against molecular length for crystalline block copolymers: (a) (\diamond) slowly cooled diblock EB and (\circ) triblock EBE copolymers; (b) (\bullet) slowly cooled triblock BEB and (\circ) triblock EBE copolymers; (c) (\bullet) self-seeded triblock BEB and (\circ) triblock EBE copolymers. The straight lines lead the eye through data sets and have no other significance.

Results and Discussion

X-ray Scattering. Scattering patterns were obtained with the samples at 10 °C. WAXS patterns were used to confirm that the E-blocks crystallized in the usual monoclinic structure with the chains packed as 7/2 helices of alternating handedness.¹¹ SAXS patterns showed evenly spaced reflections from a lamellar morphology and provided the lamellar spacings (d -spacings) used in the construction of Figure 1. In this figure, the quantity $(l/d) - 1$ is plotted against l , where l is the extended length of the copolymer calculated for E-blocks in the helical conformation (2.85 Å per E unit)¹² and B-blocks in the trans-planar conformation (3.63 Å per B unit).¹³ Assuming that the E-blocks are orientated normal to the lamellar end plane (and there is evidence to that effect from WAXS from orientated samples; see, for example ref 5), the quantity $(l/d) - 1$ provides an indication of the extent of chain folding in a sample. To maintain comparability between results for the different architectures, those obtained^{3,4} for diblock copolymers with $l < 200$ are omitted from the figure. The observation that the data points do not cluster around integral values of $(l/d) - 1$ reflects the fact that individual block lengths are important determinants of lamellar thickness, as discussed previously for diblock EB copoly-

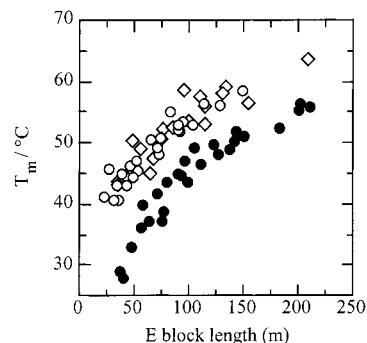


Figure 2. Dependence of melting temperature (T_m) on E-block length for (\diamond) diblock EB, (\circ) triblock EBE, and (\bullet) triblock BEB copolymers.

mers.² In the present experiments, especially for the samples crystallized by slow cooling, the measured values of d are probably averages over a range of lamellar thicknesses in the lamellar stacks. The scatter in the data points arises from variation in average block length as well as from minor variation in the crystallization process.

Results for slowly cooled diblock EB and triblock EBE copolymers are compared in Figure 1a. Within the scatter of the points these copolymers are seen to have similar extents of chain folding at a given chain length. In contrast, comparison of results for slowly cooled EBE and BEB triblock copolymers (see Figure 1b) shows that the BEB copolymer chains are significantly more folded than their EBE counterparts. One explanation is that the extent of chain folding, which during crystallization is determined kinetically by the overall chain length and the crystallization rate, is reduced by annealing after initial crystallization of the EB and EBE copolymers but that the rate of chain unfolding is much slower for the BEB copolymers. However, unlike crystalline homopolymers, the equilibrium state of a crystalline block copolymer is not necessarily the unfolded state, and it is possible that the equilibrium extent of folding is higher for BEB copolymers than for EBE copolymers. Accordingly, certain samples were crystallized within 2 °C of the measured melting point by self-seeding the melt. These results (see Figure 1c) confirmed that the slowly crystallized samples, which are more highly folded than the self-seeded samples, were not in their equilibrium state. At low chain lengths ($l < 400$ Å) the self-seeded EBE copolymers attain their unfolded conformation, whereas the self-seeded BEB copolymers attain only their once-folded conformation. It is possible that the self-seeded samples are in their equilibrium states, but this requires further investigation.

Thermal Analysis. Only the slowly cooled samples were subjected to thermal analysis. The measured melting temperature is an intrinsic quantity which can be used directly in comparison of results for the diblock and triblock copolymers. Values are compared in Figure 2 where, because the E-block is the crystallizable component, the plot is of T_m against E-block length. Within a small experimental scatter of ± 2 °C, the data points for the EB and EBE lie on a single curve while those for the BEB copolymers lie on a second curve, reflecting their lower melting points at comparable E-block length. Because a lower melting temperature means a thinner lamella (i.e., a higher extent of chain folding), this plot provides useful confirmation of the effect of block architecture on lamellar spacing described in the previous section.

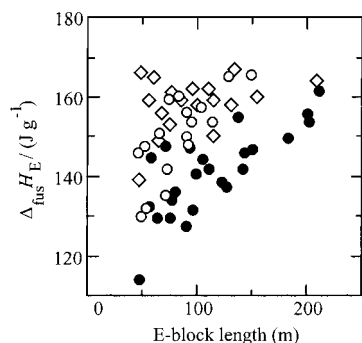


Figure 3. Dependence of enthalpy of fusion per gram of poly(oxyethylene) ($\Delta_{\text{fus}}H_E$) on E-block length for (\diamond) diblock EB, (\circ) triblock EBE, and (\bullet) triblock BEB copolymers.

In comparing the enthalpies of fusion, it is necessary to account for the mass fraction of poly(oxyethylene) in the copolymer (w_E), i.e., to calculate the enthalpy of fusion per gram of oxyethylene from

$$\Delta_{\text{fus}}H_E = \Delta_{\text{fus}}H/w_E$$

However, the overall chain length will affect the enthalpy independently of w_E , and this will impose scatter on the values of $\Delta_{\text{fus}}H_E(w_E)$. This is because a change in the overall chain length implies a change in the overall extent of chain folding and, in turn, a change in the extent of E-block folding. The fact that the entropy of fusion, $\Delta_{\text{fus}}S_E$, is affected by the extent of folding in a similar way to $\Delta_{\text{fus}}H_E$, and that

$$T_m = \Delta_{\text{fus}}H_E/\Delta_{\text{fus}}S_E$$

means that T_m is compensated against a change in the extent of chain folding and, as a consequence, provides a smooth plot against E-block length, as seen in Figure 2. $\Delta_{\text{fus}}H_E$ is plotted against E-block length in Figure 3. Data for copolymers with short E-blocks ($m < 45$ corresponding to $M_n < 2000 \text{ g mol}^{-1}$) are omitted, as $\Delta_{\text{fus}}H_E$ is particularly sensitive to folding in short chains. Even so, the data points show considerable scatter. However, there is a clear tendency for the values of $\Delta_{\text{fus}}H_E$ for the BEB copolymers to be systematically lower than those for EB and EBE copolymers.

Conclusions

Under similar crystallization conditions, lamellar crystals of triblock BEB copolymers are thinner than those of diblock EB and triblock EBE copolymers. For slowly cooled samples, this difference is attributed to the BEB chains being trapped in their kinetically determined folded conformations, the terminal B-blocks effectively reducing to zero the rate of lamellar thickening by annealing at the crystallization temperature. It is possible that samples crystallized very slowly at very low undercoolings are in their equilibrium states.

Acknowledgment. Financial support was provided by the EPSRC (UK) through Grants GR/L22621 and GR/L22645. C.C. and W.M. were supported by the Thai Government.

References and Notes

- (1) Ryan, A. J.; Mai, S.-M.; Fairclough, J. P. A.; Hamley, I. W.; Booth, C. *Phys. Chem. Chem. Phys.* **2001**, *3*, 2961.
- (2) Yang, Y.-W.; Tanodekaew, S.; Mai, S.-M.; Booth, C.; Ryan, A. J.; Bras, W.; Viras, K. *Macromolecules* **1995**, *28*, 6029.
- (3) Ryan, A. J.; Fairclough, J. P. A.; Hamley, I. W.; Mai, S.-M.; Booth, C. *Macromolecules* **1997**, *30*, 1723.
- (4) Mai, S.-M.; Fairclough, J. P. A.; Viras, K.; Gorry, P. A.; Hamley, I. W.; Ryan, A. J.; Booth, C. *Macromolecules* **1997**, *30*, 8392.
- (5) Fairclough, J. P. A.; Mai, S.-M.; Matsen, M. W.; Bras, W.; Messe, L.; Turner, S.; Gleeson, A.; Booth, C.; Hamley, I. W.; Ryan, A. J. *J. Chem. Phys.* **2001**, *114*, 5425.
- (6) Xu, J.-T.; Turner, S. C.; Fairclough, J. P. A.; Ryan, A. J.; Mai, S.-M.; Chaibundit, C.; Booth, C. *Macromolecules* **2002**, *35*, 3614.
- (7) Booth, C.; Yu, G.-E.; Nace, V. M. In *Amphiphilic Block Copolymers: Self-Assembly and Applications*; Alexandridis, P., Lindman, B., Eds.; Elsevier Science B. V.: Amsterdam, 2000; Chapter 4.
- (8) Nace, V. M.; Whitmarsh, R. H.; Edens, M. W. *J. Am. Oil Chem. Soc.* **1994**, *71*, 777.
- (9) Buckley, C. P.; Kovacs, A. J. *Prog. Colloid Polym. Sci.* **1975**, *58*, 44.
- (10) Bras, W.; Derbyshire, G. E.; Devine, A.; Clarke, S. M.; Cooke, J.; Komanschek, B.; Ryan, A. J. *J. Appl. Crystallogr.* **1995**, *28*, 26.
- (11) Takahashi, Y.; Tadokoro, H. *Macromolecules* **1973**, *6*, 881.
- (12) Craven, J. R.; Zhang, H.; Booth, C. *J. Chem. Soc., Faraday Trans.* **1991**, *87*, 1183.
- (13) Flory, P. J. *Statistical Mechanics of Chain Molecules*; Interscience: New York, 1969; p 165.

MA0201680